Catalytic Conversion of Sugars from Coffee Waste and Xylose into Furfural over Fe/SiO2 Catalysts

Kevin René Suárez , William Giovanni Cortés-Ortiz , Carlos Alberto Guerrero-Fajardo *

Posted Date: 13 February 2025

doi: 10.20944/preprints202502.0814.v1

Keywords: heterogeneous catalysis; furfural production; sol-gel synthesis; residual biomass valorization

 doi:10.20944/preprints202502.0814.v1

Article

Catalytic Conversion of Sugars from Coffee Waste and Xylose into Furfural over Fe/SiO2 Catalysts

Kevin Suárez [1], William Cortés-Ortiz [1] and Carlos Guerrero-Fajardo [2,*]

[1] Departamento de Química, Química Farmacéutica, Universidad El Bosque, Bogotá DC, 11001, Colombia

[2] Departamento de Química, Facultad de Ciencias, Grupo APRENA, Universidad Nacional de Colombia, Sede Bogotá, Bogotá DC 11001, Colombia

* Correspondence: caguerrerofa@unal.edu.co

Abstract: Solid Fe catalysts supported on SiO_2 with Lewis and Brönsted acidity were synthesized using the sol-gel methodology. FTIR spectroscopy, XRD, Raman spectroscopy, BET isotherms, and SEM characterized the materials. Subsequently, they were used to dehydrate xylose to obtain furfural. It was observed that increasing the metal loading from 0.5 % to 1.5 % by mass increases the selectivity to furfural up to 40.09 %; in addition to this, it was observed that the calcination temperature has an effect concerning the conversion since the materials calcined at 450 °C present higher xylose conversion concerning the materials calcined at 750 °C. Finally, it was observed that the catalysts are active and effective in obtaining furfural from hydrolysates obtained from hydrothermal treatments of the residual biomass of the coffee crop, obtaining an average of 9.11 mg/g of furfural per gram of biomass.

Keywords: heterogeneous catalysis; furfural production; sol-gel synthesis; residual biomass valorization

1. Introduction

Coffee is one of the agricultural products with the highest consumption globally, and it is the leading exporter in Vietnam, Brazil, and Colombia [1]. According to the International Coffee Organization, in September 2022, there was an increase in exports of 9.95 million bags, with Colombia being one of the main protagonists worldwide [2]. Based on the above, the high production of coffee brings a large amount of waste, usually used for one of the following activities: i) fertilizer for crops, ii) disposal as solid waste on farms, or iii) incineration.

Once the coffee is collected from the plants, a process begins before it reaches homes to be consumed. This process is divided into the following stages. i) Pulped consists of removing the coffee's soft part (cherry), generally accompanied by washing and, therefore, a high-water consumption. ii) Drying: once the cherry is removed from the coffee, a drying process begins until it has a moisture percentage of around 10 %. In Colombia, this process is carried out in the sun in structures called heldas. iii) Roasting: once dry, the coffee is transported to places where it is roasted at temperatures close to 200 °C. During this process, the coffee's physical and chemical properties are modified, giving it its characteristic flavor at the end. Finally, iv) it is transported and packaged for distribution.

Based on the above and the high amount of waste generated during the coffee harvest, the option of using biomass waste as raw material for the production of chemicals of commercial interest has been evaluated [3]. To use biomass waste, which is composed mainly of three fractions: cellulose, hemicellulose, and lignin, as raw material, mechanical, physical, and chemical treatments must be applied. The treatments allow the biomass to be fractionated and to access monomeric sugars, starting molecules for obtaining products of industrial value [4].

 doi:10.20944/preprints202502.0814.v1

Thus, furfural is one of the products of interest that can be obtained from coffee waste. Furfural is a vital chemical obtained from agricultural or forestry residues rich in polymers of five-carbon sugars [5]. In the same way, furfural is one of the platform chemicals obtained from biomass that can be converted into various useful products used in the pharmaceutical, fine chemical, petroleum refining, agrochemical, biofuels, and polymer industries [6].

Usually, furfural is obtained from biomass by using strong mineral acids. Specifically, sulfuric acid hydrolyzes biomass and dehydrates xylose to furfural. This process, although it generates excellent yields, also brings with it several drawbacks of which it stands out: i) high production of acidic wastewater, corrosion of equipment, iii) difficulty of separation of the product of interest, and i) high formation of by-products [7]. Based on the above, the use of solid catalytic materials to obtain furfural from xylose has been evaluated. In this regard, the proposed mechanism involves two steps. The first is the isomerization of xylose to xylulose mediated by Lewis acid sites, and the second is the dehydration of xylulose to furfural attributed to Brönsted acid sites [8].

On the other hand, solid materials have been evaluated as catalysts. In this sense, furfural yield values around 53 % have been reported using $two SO_4^{2-}/ZrO_2 - Al_2O_3/SBA - 15$ At 160 °C for four h, suggesting the importance of the catalysts' acid sites [9]. Likewise, using iron catalytic materials supported on activated carbon, values around 57 % of yield associated with iron oxide species have been reported [10].

Thus, this research initially characterized residual biomass of coffee cultivation in terms of moisture content, ash, and total solids. In the same way, the percentage of cellulose, hemicellulose, and lignin was determined. Subsequently, hydrothermal treatment was applied to the biomass to evaluate obtaining xylose and furfural. Finally, catalytic iron materials were assessed for the dehydration of xylose commercial and the xylose obtained from the hydrolysates of coffee residues, thus determining the conversion percentages, selectivity, and yield.

Regarding the catalytic materials evaluated, mesoporous iron catalysts supported in silica were prepared and characterized using the sol-gel method. During the synthesis were evaluated two iron charges, 0.5 and 1.5 wt %, and two calcination temperatures, 450 and 750 °C, named 0,5Fe-Si-450, 0,5Fe-Si-750, 1,5Fe-Si-450 y 1,5Fe-Si-750, respectively. In this way, iron species act as Lewis acid sites; hence, it is essential to evaluate two different loads to identify their role in the catalytic process of dehydration from xylose to furfural. On the other hand, the calcination temperature influences the type of iron species that form a mixture of calcined materials at 750 °C, allowing iron oxides type hematite with Fe^{3+}. Based on the above, this work presents a successful case of obtaining a platform molecule, furfural, from agricultural coffee residues using solid acid catalysts.

2. Materials and Methods

2.1. Biomass Material

The residual coffee biomass was collected from a Puente Nacional, Colombia private farm. The percentage of humidity was determined following the NREL/TP-510-42621 standard proposed by the National Renewable Energy Laboratory [11]. In the same way, as with dry biomass, the percentage of ash was determined following the NREL/TP-510-42622 protocol proposed by the National Renewable Energy Laboratory [12]. Finally, cellulose, hemicellulose, and lignin were determined following the NREL/TP-510-42618 protocol proposed by the National Renewable Energy Laboratory [13].

2.2. Hydrothermal Treatment of Biomass

The hydrothermal treatments applied to the residual coffee biomass were carried out in a stainless steel reactor in a nitrogen atmosphere. A typical test loaded 5.00 g of biomass and 100 mL of water into the reactor. Subsequently, the treatment temperature is programmed, 170 or 190 ° C, and the agitation begins at 500 rpm; once the programmed temperature is reached, the time starts to run, 30 or 60 minutes. Once the treatment is finished, the reactor is cooled for one hour to room

 doi:10.20944/preprints202502.0814.v1

temperature and then goes into an ice bath. Finally, the solid is separated, and the hydrolysate is analyzed by high-efficiency liquid chromatography (HPLC) to quantify xylose and furfural.

2.3. Catalysts Preparation

The iron catalysts supported in silicon oxide were prepared according to the procedure described in another article of our research group [14]. All reagents used were analytical grade obtained from Sigma-Aldrich. Tetraethyl orthosilicate (TEOS 98 %) and iron acetate (99 %) were used as precursors for silicon and iron, respectively. On the other hand, oxalic acid (99 %) was used as a structure-directing agent. For the synthesis of catalysts, a defined mass of oxalic acid was mixed in ethanol and stirred vigorously to obtain a homogeneous solution. Moreover, the iron precursor required to obtain materials with iron charges of 0.5 and 1.5 wt % was dissolved in ethanol. These two solutions were added to another container containing TEOS. Finally, water was added according to the ratio 1/1/4 TEOS/oxalic acid/water. Once the solution was formed, the gelation process was carried out at 70 ° C for 7 hours with a stirring of 300 rpm. After this time, the materials were dried at 105 °C for 12 hours and calcined at 450 or 750 °C for 6 hours.

2.4. Characterization of Catalysts

X-ray diffraction patterns were obtained on a Rigaku diffractometer with a Cu anode and a nominal current tube voltage of 45 kV. Data were collected at room temperature between 10° and 90° with a geometry of 2θ. The infrared spectra (FTIR) were recorded on a Nicolet FTIR iS10 spectrophotometer. The spectra were determined in the 4000–400 cm^{-1} spectral range. Transmission spectra were obtained from the samples diluted with KBr; the tablet was prepared with around 1 mg of the sample solid and 200 mg of pure KBr. All the spectra were recorded at a resolution of 2 cm^{-1}.

Raman spectra were obtained using a Thermo Scientific Raman microscope with 540 nm excitation from a diode laser through a ×10 objective. The scattered radiation from the sample was collected at right angles to the laser beam and was directed to a detector with a photodiode array of thermoelectric cooled to −48 °C. Adsorption–desorption isotherms were carried out in a Quantachrome Autosorb sorptometer, employing N_2 as the adsorbent. Samples (200 mg) were degassed for six hours at 200 °C before analysis. The specific surface area was calculated using the standard Brunauer-Emmett-Teller (BET method) based on adsorption data in a relative pressure range from 0.07<P/Po<0,3. Finally, the physical appearance of the catalysts was obtained by scanning electron microscopy (SEM) using Jeol equipment, JSM7100F a 10000x.

2.5. Catalytic Conversion of Xylose and Coffee Waste to Furfural

The catalytic tests were conducted in a batch reactor of stainless steel and nitrogen atmosphere. In a typical procedure, 100 mL of aqueous xylose solution and 100 mg of catalyst are placed inside the reactor. The catalytic system is purged with nitrogen three times, and the reaction mixture is rapidly heated to 170 or 190 °C under 500 rpm stirring. When the programmed temperature is reached, the zero time is taken, and the reaction is allowed for 30, 60, or 120 min. Once the response is over, the reactor is cooled for one hour to room temperature and then placed in an ice bath. Finally, the catalyst is separated, and the liquid is analyzed by high-efficiency liquid chromatography (HPLC) to quantify xylose and furfural. The same procedure is performed with the hydrolysates of the biomass treatment. Thus, 100 mL of the hydrolysate obtained from the hydrothermal treatment and 100 mg of catalyst are placed inside the reactor. The temperature and agitation are programmed. Once the reaction is finished, the catalyst is separated from the liquid, which is used to quantify xylose and furfural by HPLC.

2.6. Xylose an Furfural Quantification

After the reaction, the aqueous phase is filtered, and the concentration of furfural present is quantified in a chromatographic equipment SHIMADZU Prominence-i LC2030, equipped with a UV

 doi:10.20944/preprints202502.0814.v1

detector and an Optiacua PUR 100 C18 column of 3 µm. The detection and quantification of furfural was developed at 275 nm, using an internal standard furfuryl alcohol that is absorbed at 210 nm. A RID 20 detector and a chromatographic column VDSpher® PUR 100 HILIC-SAC are used to quantify xylose, using inositol as an internal standard.

3. Results and Analysis

3.1. Coffee Waste Biomass

The residual biomass of coffee used is from the pulping process or pulping of the fruit. Thus, Table 1 presents the results of the percentage of moisture, ash, cellulose, hemicellulose, and lignin compared with the results obtained by other authors.

Table 1. Physicochemical characterization (% w/w dry).

Component	This work	[1]	[15]	[16]
Moisture	3,11 ± 0,0061	9,11 ± 0,39	4,12	11,00
ashes	7,60 ± 0,064	0,96 ± 0,13	2,27	1,27 ± 0,03
Cellulose	19,60 ± 0,59	35,13 ± 0,81	37,35	40,39 ± 2,20
Hemicellulose	14,90 ± 0,45	11,42 ± 0,31	27,79	34,01 ± 1,20
Lignin	16,90 ± 0,51	23,27 ± 0,25	19,81	10,13 ± 1,30

As can be seen, the reported values have the same tendency as those obtained in the present work. However, the differences presented were attributed to three main aspects: i) the separation of each of the residual components of coffee, ii) the variety of coffee used, and iii) the particular cultivation conditions. For the specific case, the interest focuses on the amount of hemicellulose since it is a polymer composed of pentoses, the raw material for obtaining furfural [17].

Once the biomass was characterized, hydrothermal treatments were applied to evaluate the influence of temperature and time on the amount of xylose and furfural. Thus, Figure 1 shows the amount of xylose and furfural obtained from residual coffee biomass.

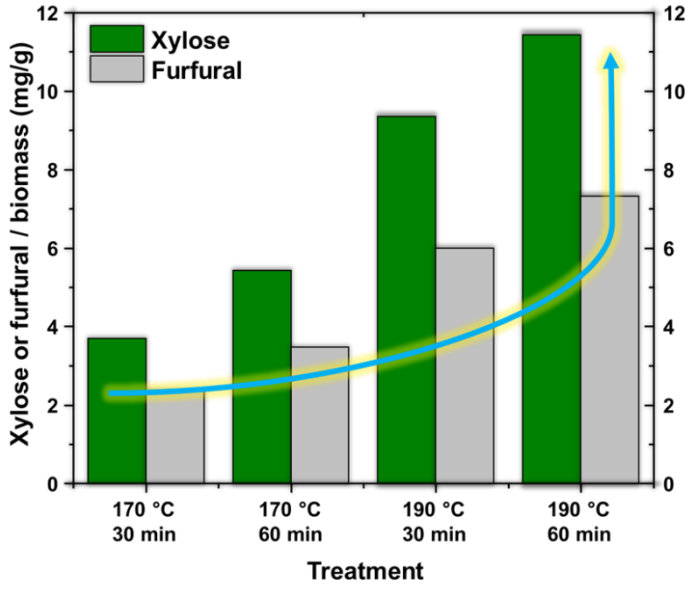

Figure 1. Influence of temperature and time in obtaining xylose and furfural.

Figure 1 shows the direct influence of temperature and hydrothermal treatment time in obtaining xylose and furfural. For xylose, it is observed that at 170 °C, increasing the time generates an increase in obtaining sugar, mainly attributed to the influence of reaction time on the hydrolysis

 doi:10.20944/preprints202502.0814.v1

of hemicellulose. The same trend is observed for furfural, only in a smaller proportion. On the other hand, increasing the temperature to 190 °C and a time of 30 min generates an increase of a little more than double in the production of xylose from coffee waste. Under these same conditions, the production of furfural triples. This is attributed to the influence of temperature, which generates the breaking of glycosidic bonds, thus obtaining monomers of sugars (xylose), which are subsequently dehydrated for the formation of furfural [18].

It is important to note that, although an increase in time allows greater obtaining of both xylose and furfural at the two temperatures evaluated, its incidence is not as relevant as the increase in temperature. Thus, it can be determined that the molecules move greater at higher temperatures, influencing the hydrolysis process of hemicellulose. In the same way, hydrothermal treatment is mainly a hybrid treatment between a physical process and a chemical process; for the specific case, the water is in a subcritical state, which promotes its action as Brönsted acid and allows the hydrolysis of biomass [19].

3.2. Characterization of Catalysts

The catalysts were characterized by XRD, FT-IR, Raman, SEM, and optometry to identify the influence of the calcination temperature on their synthesis. The XRD patterns are shown in Figure 2.

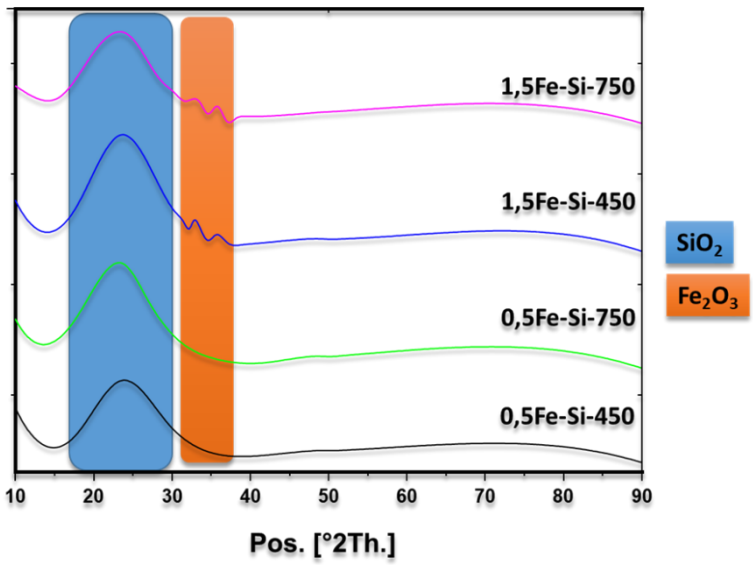

Figure 2. XRD patterns of iron catalysts.

Figure 2 shows a broad peak at 2θ = 22 °, which is assigned to amorphous silica [20], [21], [22]. On the other hand, no peaks attributed to iron species are observed for materials with an iron charge of 0.5 wt % (0.5Fe-450 and 0.5Fe-750). This is due to the high degree of dispersion of active species associated with the process of sol-gel synthesis. As for materials with an iron charge of 1.5 wt % (1.5Fe-450, 1.5Fe-750) in addition, the broad peak of silica is observed in two peaks at 2θ = 33 and 35 ° which can be assigned to species of iron oxide type hematite JCPDS: 33-0664 [23], [24], [25]. It is essential to highlight the presence of hematite-type iron in which the metal has oxidation state Fe^{3+} [26]. For the particular reaction of dehydration of xylose to furfural, Fe^{3+} will act as Lewis acid, promoting the isomerization of xylose to xylulose.

Figure 3 shows FT-IR spectra of the synthesized catalysts in a range of 4000-500 cm^{-1}. The peak around 3500 cm^{-1} can be explained by the modes of extension of OH groups [20], [27]. Such OH groups can be bonded to a hydrogen atom, HO-H, or a silicon atom, forming Si-OH. Si-OH has a vital role in a catalytic process. Although many authors suggest that it is inert to the supports in the catalysts, this OH group attached to the support can act as Brönsted acid, favoring the dehydration of xylulose to furfural.

 doi:10.20944/preprints202502.0814.v1

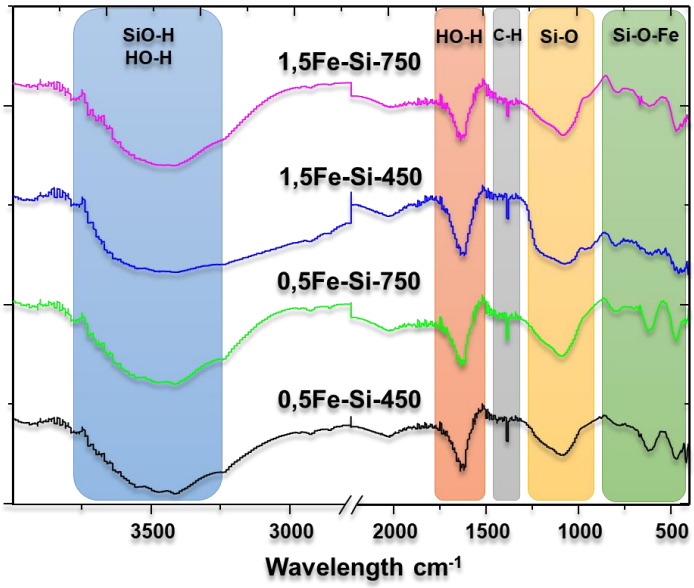

Figure 3. FT-IR spectra of iron catalysts.

The broadband around 3500 cm^{-1} can be considered composed of a superposition of SiO-H extension [28]. Table 2 details the wavelengths and their assignments.

Table 2. FT-IR band assignment around 3500$cm^{-1.}$

Wavelength (cm^{-1})	Assignment
3750	Isolated neighborhood SiO-H extension
3660	Extension of hydrogen bond SiO-H or internal SiO-H extension
3540	SiO-H extension of surface silanol groups bonded by hydrogen to molecular water
3500-3400	O-H extension of hydrogen bonded to molecular water

On the other hand, the band is highlighted at 1082 $cm^{-1,}$ which is attributed to Si-O-Si extension vibrations [29], [30]. In the same way, one shoulder is observed around 1200 cm^{-1} due to the vibration of the extension of the Si-O bond, and another small band is observed at 981 cm^{-1} due to the Si-O bond in the Si-OH silanol groups [31]. Likewise, 461 and 798 cm^{-1} bands are assigned to the Si-O-Si bond ring structure [32].

Figure 4 shows the Raman peaks of the synthesized iron materials. An intense peak is around 1300 cm^{-1}, associated with hematite-type iron species [33]. In this regard, greater intensity is observed in materials synthesized at 750 °C than those calcined at 450 °C. This is attributed to the more significant number of species formed at 750 °C, the temperature at which iron mostly has an oxidation state Fe^{3+}. At 450 °C, there is a mixture of iron Fe^{2+} and Fe^{3+}. In the same way, peaks are observed at 225, 245, 292, 390, 500, 615, and 960, all associated with hematite-type iron [34], [35]. Based on the above, the presence of iron is complemented and confirmed by its higher oxidation state, which acts as Lewis acid during the dehydration reaction of xylose to furfural.

 doi:10.20944/preprints202502.0814.v1

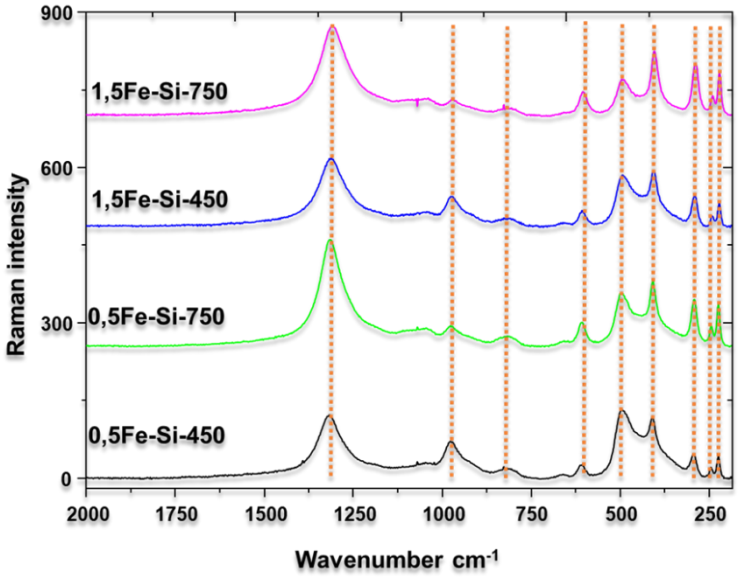

Figure 4. Raman spectra of iron catalysts.

The adsorption and desorption isotherms of iron materials supported on silicon oxide are presented in Figure 5. Bearing in mind that during nitrogen adsorption at pressures lower than 0.1 ($p/p0 < 0.1$), a filling of the surface by a monolayer of N_2 [36], [37]; a line was drawn at this relative pressure to identify the adsorbed volume of N_2 and relate it to the synthesis conditions of each material. Type II isotherms are observed when comparing the samples calcined at 450 °C with a load of 0.5 and 1.5 % in mol of iron (Figure 4a and 4b) [37]. In this case, the surface is 730 and 693 m^2/g, respectively. Based on the surface area values, it can be seen that the sample with the lowest iron load and calcined at 450 °C (0.5Fe-450) required a more significant amount of nitrogen to fill the monolayer (8,49 mmol/g). The material with the highest load and calcined at the same temperature (1.5Fe-450) required 8,05 mmol/g of N_2. This allows us to observe the influence of iron loading on the structural formation of the silicon lattice. The higher iron loading leads to structures with lower area due to the higher formation of Si-O-Fe bonds.

On the other hand, the catalysts calcined at 750 °C (0.5Fe-750 and 1.5Fe-750) present lower surface area values and, therefore, lower N_2 expenditure for monolayer fill. Thus, areas of 569 and 579 m^2/g and nitrogen values of 6,48 and 7,57 mmol/g are observed, respectively. The lower values of area and N_2 expenditure are attributed to the calcination temperature since it influences both the decrease in the surface area and the pore diameter, causing loss of chemically bound water, ii) reduction of silanol groups (Si-OH), which generates a contraction of the material structure, iii) modification of the texture by sintering [38]. In this aspect, tiny crystals or particles become larger structures due to the decrease in surface energy caused by the reduction of surface area and the elimination of solid interfaces. Thus, the final structure resulting from the sintering process generates grain growth and decreases pore size.

In general, SEM images show materials with angular shapes characteristic of silica [29]. In the same way, an amorphous structure with agglomerates is observed in all cases, which is also characteristic of silica materials prepared by the sol-gel method [22]. Likewise, irregular shapes of different sizes are observed, in which a defined microstructure is not identified.

 doi:10.20944/preprints202502.0814.v1

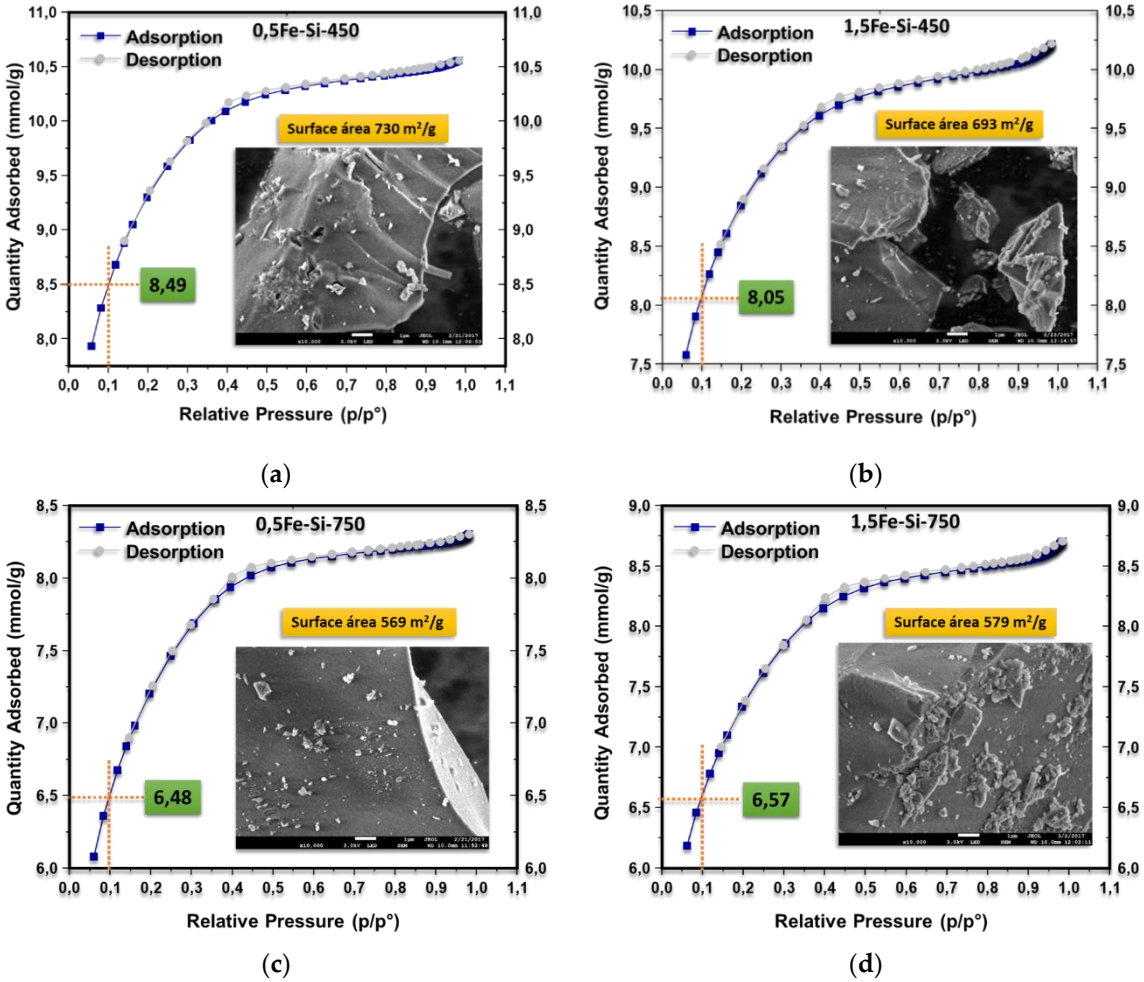

Figure 5. N_2 adsorption-desorption isotherms of iron catalysts. catalyst 0,5Fe-Si-450 (a), catalyst 1,5Fe-Si-450 (b), catalyst 0,5Fe-Si-750 (c), and catalyst 1,5Fe-Si-750 (d).

3.3. Production of Furfural from Xylose

The effect of iron loading and calcination temperature of materials on xylose to furfural dehydration at 170 °C and 120 minutes is shown in Figure 6. Without a catalyst, a xylose conversion of 59.82% in mol and a selectivity of 21.17% in mol are observed. In this aspect, it is essential to emphasize that at 170 ° C in a pressurized system, the water acts as acid, generating the dehydration of the xylose [39], [40]. As for iron materials, all generate higher values of selectivity to furfural and, therefore, process performance. In this regard, iron catalysts, supported by silicon oxide, fulfill a double function. The hydrogen of the silane groups of the support (Si-OH) act as Brönsted acid, promoting the isomerization of xylose to xylulose [41]. On the other hand, the active centers of iron (Fe^{3+}) act as Lewis acid, generating the dehydration of xylulose and the formation of furfural [42].

 doi:10.20944/preprints202502.0814.v1

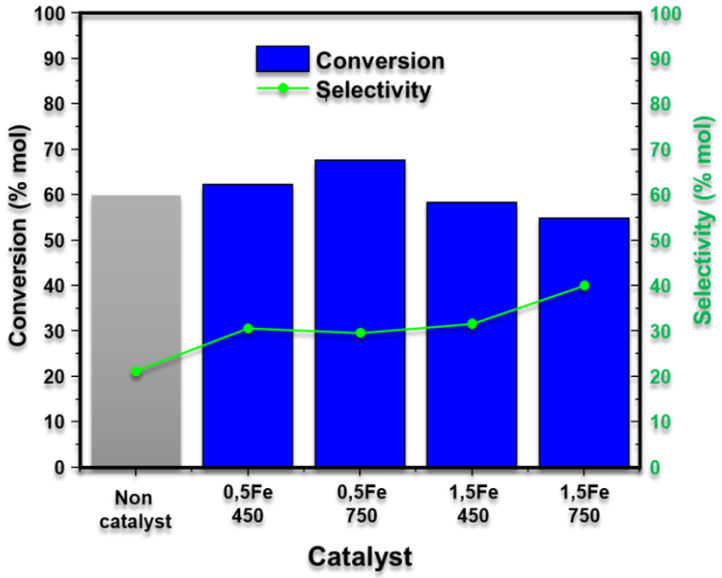

Figure 6. Xylose conversion and furfural selectivity of iron catalysts.

Figure 6 shows that regardless of the calcination temperature, the highest iron load (1.5Fe-450 and 1.5Fe-750) generates the lowest values of xylose conversion, 58.27 and 54.76 % in mole. However, this higher iron load generates the highest selectivity to furfural, 31.62 and 40.09 % in mol. In this way, the higher iron load decreases the number of silanol groups (Si-OH) and, therefore, the activation and initial conversion of xylose. However, this higher iron load generates more active iron centers, which favor the formation of furfural. Likewise, comparing the calcination temperature between materials with higher iron load (1.5Fe-450 and 1.5Fe-750), it is observed that the catalyst calcined at 750 °C is more selective towards furfural, 40.09 % in mol. This allows us to recognize that the higher calcination temperature promotes the formation of hematite-type iron species (Fe^{3+}), which act as Lewis acid and favor the formation of furfural [43], [44].

The effect of surface area on xylose conversion and yield to furfural is presented in Figure 7. In this regard, it is highlighted that the material with the most significant area (730 m2 / g) is obtained at the lowest calcination temperature (450 ° C), has a low iron load (0.5Fe-450), and generates a conversion of xylose and selectivity to furfural of 62.14 and 30.61 % in mol, respectively. In this way, a larger surface area maximizes the access of the reagents, promotes collisions between them, and influences the selectivity of the process.

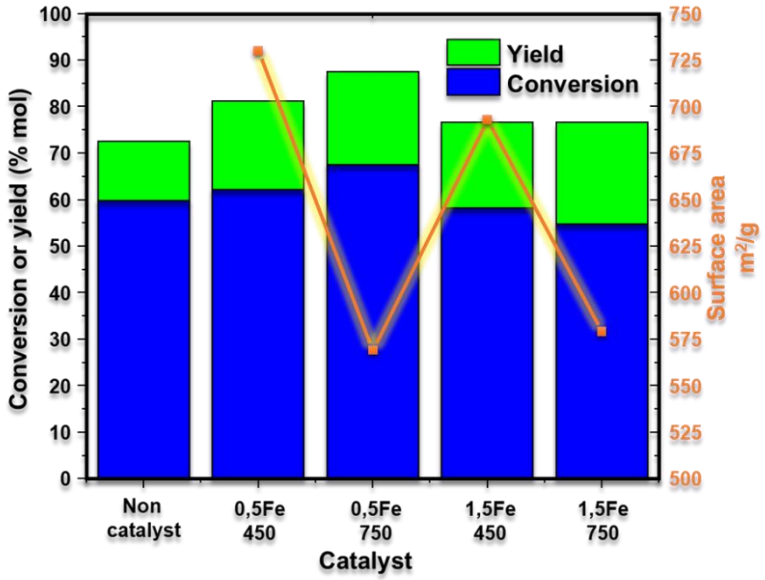

 doi:10.20944/preprints202502.0814.v1

Figure 7. Xylose conversion and yield of iron catalysts.

3.4. Production of Furfural from Coffee Residual Biomass Hydrolysates

Once the residual coffee biomass has been hydrothermally treated, xylose will be used as a raw material to obtain furfural (1,5Fe-750) based on the results of the best catalyst. Catalytic reactions were carried out at 170 °C for two hours, each hydrolysate containing 100 mg of catalyst. The results are presented in Figure 8.

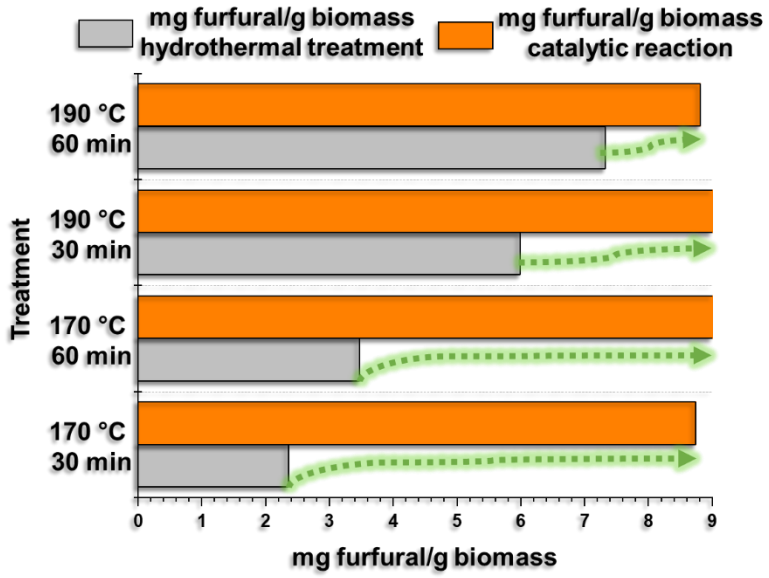

Figure 8. Variation of the furfural production between hydrothermal treatment vs catalytic reaction.

Based on Figure 8, when carrying out the catalytic reaction at 170 °C for two h with each of the hydrolyzates and using the catalyst with the highest iron load 1.5 wt % and calcined at 750 °C (1.5 - Fe-750), the amount of furfural obtained increases in all tests. In this sense, as previously mentioned, the biomass was subjected to hydrothermal treatments at 170 and 190 °C for 30 or 60 minutes, which, in addition to producing xylose, allowed furfural to be obtained. However, when using the hydrolysates obtained at 170 °C (30 and 60 minutes) and the iron catalyst, an increase in furfural production was generated, going from 2.36 to 8.74 mg of furfural/g of biomass and from 3.47 to 9.63 mg of furfural/g of biomass, respectively. This is attributed to the catalytic role of iron species (Lewis acid) and silanol groups (Brönsted acids).

Regarding the hydrolysates obtained at 190 °C (30 and 60 minutes), it is observed that the hydrothermal process carried out for 30 minutes and then catalytically for two h, generates an increase in furfural production from 5.99 to 9.26 mg. of furfural/g of biomass and from 7.32 to 8.81 mg. Based on the above, it can be seen that in all cases, furfural production was increased by using an iron catalyst supported by silicon oxide. The most significant increases are observed in the hydrolysates obtained at a lower temperature (170 °C) than those obtained at 190 °C.

4. Conclusions

Based on Figure 8, when carrying out the catalytic reaction at 170 °C for two h with each of the hydrolyzates and using the catalyst with the highest iron load 1.5 wt % and calcined at 750 °C (1.5 - Fe-750), the amount of furfural obtained increases in all tests. In this sense, as previously mentioned, the biomass was subjected to hydrothermal treatments at 170 and 190 °C for 30 or 60 minutes, which, in addition to producing xylose, allowed furfural to be obtained. However, when using the hydrolysates obtained at 170 °C (30 and 60 minutes) and the iron catalyst, an increase in furfural production was generated, going from 2.36 to 8.74 mg of furfural/g of biomass and from 3.47 to 9.63

 doi:10.20944/preprints202502.0814.v1

mg of furfural/g of biomass, respectively. This is attributed to the catalytic role of iron species (Lewis acid) and silanol groups (Brönsted acids).

Regarding the hydrolysates obtained at 190 °C (30 and 60 minutes), it is observed that the hydrothermal process carried out for 30 minutes and then catalytically for two h, generates an increase in furfural production from 5.99 to 9.26 mg. of furfural/g of biomass and from 7.32 to 8.81 mg. Based on the above, it can be seen that in all cases, furfural production was increased by using an iron catalyst supported by silicon oxide. The most significant increases are observed in the hydrolysates obtained at a lower temperature (170 °C) than those obtained at 190 °C.

Data Availability Statement: The original contributions presented in this study are included in the article. Further inquiries can be directed to the corresponding author.

Acknowledgments: The authors want to acknowledge Universidad Nacional de Colombia and Universidad El Bosque for funding projects.

Conflicts of Interest: The authors declare no conflicts of interest.

References

1. V. Aristizábal-Marulanda, J. A. Poveda-Giraldo, and C. A. Cardona Alzate, "Comparison of furfural and biogas production using pentoses as a platform," *Science of the Total Environment*, vol. 728, pp. 1–12, 2020, doi: 10.1016/j.scitotenv.2020.138841.
2. "International Coffee Organization - What's New." Accessed: Nov. 01, 2022. [Online]. Available: https://www.ico.org/
3. Y. Piñeros-castro, G. A. Velasco, W. G. Cortes Ortiz, and J. Proaños, "Producción de azúcares fermentables por hidrólisis enzimática de cascarilla de arroz pretratada mediante explosión con vapor," *Revista Ión*, vol. 24, no. 2, pp. 23–28, 2011.
4. W. G. Cortés Ortiz, "Tratamientos Aplicables a Materiales Lignocelulósicos para la Obtención de Etanol y Productos Químicos," *Revista de Tecnología*, vol. 13, no. 1, pp. 39–44, 2014.
5. B. Pholjaroen, N. Li, Z. Wang, A. Wang, and T. Zhang, "Dehydration of xylose to furfural over niobium phosphate catalyst in biphasic solvent system," *Journal of Energy Chemistry*, vol. 22, no. 6, pp. 826–832, 2013, doi: 10.1016/S2095-4956(14)60260-6.
6. N. W. Dulie, B. Woldeyes, and H. D. Demsash, "Synthesis of lignin-carbohydrate complex-based catalyst from Eragrostis tef straw and its catalytic performance in xylose dehydration to furfural," *Int J Biol Macromol*, vol. 171, pp. 10–16, Feb. 2021, doi: 10.1016/J.IJBIOMAC.2020.12.213.
7. N. Zhou et al., "Conversion of xylose into furfural over MC-SnOx and NaCl catalysts in a biphasic system," *J Clean Prod*, vol. 311, no. June, p. 127780, 2021, doi: 10.1016/j.jclepro.2021.127780.
8. R. Ji et al., "Core-shell catalyst WO3@mSiO2-SO3H interfacial synergy catalyzed the preparation of furfural from xylose," *Molecular Catalysis*, vol. 530, no. July, 2022, doi: 10.1016/j.mcat.2022.112592.
9. X. Shi, Y. Wu, P. Li, H. Yi, M. Yang, and G. Wang, "Catalytic conversion of xylose to furfural over the solid acid SO 42-/ZrO2-Al2O3/SBA-15 catalysts," *Carbohydr Res*, vol. 346, no. 4, pp. 480–487, Mar. 2011, doi: 10.1016/j.carres.2011.01.001.
10. A. Rusanen, R. Kupila, K. Lappalainen, J. Kärkkäinen, T. Hu, and U. Lassi, "Conversion of xylose to furfural over lignin-based activated carbon-supported iron catalysts," *Catalysts*, vol. 10, no. 8, 2020, doi: 10.3390/catal10080821.
11. A. Sluiter et al., "Determination of total solids in biomass and total dissolved solids in liquid process samples," *National Renewable Energy Laboratory (NREL)*, no. March, pp. 3–5, 2008, doi: NREL/TP-510-42621.
12. A. Sluiter, B. Hames, R. Ruiz, C. Scarlata, J. Sluiter, and D. Templeton, "Determination of Ash in Biomass Laboratory Analytical Procedure (LAP) Issue Date : 7 / 17 / 2005 Determination of Ash in Biomass Laboratory Analytical Procedure (LAP)," no. January, 2008.
13. A. Sluiter, B. Hames, R. Ruiz, and C. Scarlata, "Determination of structural carbohydrates and lignin in biomass," *Laboratory analytical …*, vol. 2011, no. July, 2008.

 doi:10.20944/preprints202502.0814.v1

14. W. G. Cortés Ortiz et al., "Partial oxidation of methane and methanol on FeOx- , MoOx- and FeMoOx -SiO 2 catalysts prepared by sol-gel method : A comparative study," *Molecular Catalysis*, vol. 491, no. February, p. 110982, 2020, doi: 10.1016/j.mcat.2020.110982.
15. J. A. Quintero, J. Moncada, and C. A. Cardona, "Techno-economic analysis of bioethanol production from lignocellulosic residues in Colombia: A process simulation approach," *Bioresource Technology*, vol. 139, pp. 300–307, 2013, doi: 10.1016/j.biortech.2013.04.048.
16. V. Aristizábal M., Á. Gómez P., and C. A. Cardona A., "Biorefineries based on coffee cut-stems and sugarcane bagasse: Furan-based compounds and alkanes as interesting products," *Bioresource Technology*, vol. 196, pp. 480–489, 2015, doi: 10.1016/j.biortech.2015.07.057.
17. L. Zhang, G. Xi, J. Zhang, H. Yu, and X. Wang, "Efficient catalytic system for the direct transformation of lignocellulosic biomass to furfural and 5-hydroxymethylfurfural," *Bioresource Technology*, vol. 224, pp. 656–661, 2017, doi: 10.1016/j.biortech.2016.11.097.
18. J. Y. Zhu and X. Pan, "Efficient sugar production from plant biomass: Current status, challenges, and future directions," *Renewable and Sustainable Energy Reviews*, vol. 164, no. April, p. 112583, 2022, doi: 10.1016/j.rser.2022.112583.
19. T. R. Sarker, F. Pattnaik, S. Nanda, A. K. Dalai, V. Meda, and S. Naik, "Hydrothermal pretreatment technologies for lignocellulosic biomass: A review of steam explosion and subcritical water hydrolysis," *Chemosphere*, vol. 284, no. June, p. 131372, 2021, doi: 10.1016/j.chemosphere.2021.131372.
20. F. Adam and A. Iqbal, "Silica supported amorphous molybdenum catalysts prepared via sol-gel method and its catalytic activity," *Microporous and Mesoporous Materials*, vol. 141, no. 1–3, pp. 119–127, 2011, doi: 10.1016/j.micromeso.2010.10.037.
21. W. G. Cortés Ortiz, A. Baena Novoa, and C. A. Guerrero Fajardo, "Structuring-agent role in physical and chemical properties of Mo/SiO2 catalysts by sol-gel method," *Journal of Sol-Gel Science and Technology*, vol. 89, no. 2, pp. 416–425, 2019, doi: 10.1007/s10971-018-4892-7.
22. C. A. Guerrero Fajardo, Y. N'Guyen, C. Courson, and A.-C. Roger, "Fe/SiO2 catalysts for the selective oxidation of methane to formaldehyde," *Ingeniería e Investigación*, vol. 26, no. 2, pp. 37–44, 2006.
23. A. Alayat, D. N. Mcllroy, and A. McDonald, "Effect of synthesis and activation methods on the catalytic properties of silica nanospring (NS)-supported iron catalyst for Fischer-Tropsch synthesis," *Fuel Processing Technology*, vol. 169, pp. 132–141, Jan. 2018, doi: 10.1016/J.FUPROC.2017.09.011.
24. S. Liu, K. Yao, L.-H. Fu, and M.-G. Ma, "Selective synthesis of Fe 3 O 4 , γ-Fe 2 O 3 , and α-Fe 2 O 3 using cellulose-based composites as precursors," *RSC Adv.*, vol. 6, no. 3, pp. 2135–2140, 2016, doi: 10.1039/C5RA22985E.
25. X. Zhang, Y. Niu, X. Meng, Y. Li, and J. Zhao, "Structural evolution and characteristics of the phase transformations between α-Fe2O3, Fe3O4 and γ-Fe2O3 nanoparticles under reducing and oxidizing atmospheres," *CrystEngComm*, vol. 15, no. 40, p. 8166, 2013, doi: 10.1039/c3ce41269e.
26. G. S. Parkinson, "Iron oxide surfaces," *Surface Science Reports*, vol. 71, no. 1, pp. 272–365, Mar. 2016, doi: 10.1016/j.surfrep.2016.02.001.
27. V. K. Vyas et al., "Assessment of nickel oxide substituted bioactive glass-ceramic on in vitro bioactivity and mechanical properties," *Boletín de la Sociedad Española de Cerámica y Vidrio*, vol. 55, no. 6, pp. 228–238, Nov. 2016, doi: 10.1016/J.BSECV.2016.09.005.
28. C. J. Brinker and G. Scherer, "Structural Evolution during Consolidation," in *Sol-Gel Science*, San Diego: Academic Press, 1990, ch. 9, pp. 514–615. doi: //doi.org/10.1016/B978-0-08-057103-4.50014-3.
29. M. Pudukudy and Z. Yaakob, "Methane decomposition over Ni, Co and Fe based monometallic catalysts," *Chemical Engineering Journal*, vol. 262, pp. 1009–1021, 2015.
30. K. Khalil and S. Makhlouf, "High surface area thermally stabilized porous iron oxide/silica nanocomposites via a formamide modified sol–gel process," *Applied Surface Science*, vol. 254, no. 13, pp. 3767–3773, Apr. 2008, doi: 10.1016/J.APSUSC.2007.11.066.
31. Z. Zhan and H. C. Zeng, "A catalyst-free approach for sol–gel synthesis of highly mixed ZrO2–SiO2 oxides," *Journal of Non-Crystalline Solids*, vol. 243, pp. 26–38, 1999, doi: 10.1016/S0022-3093(98)00810-2.

 doi:10.20944/preprints202502.0814.v1

32. R. Neumann and M. Levin-Elad, "Metal Oxide (TiO2, MoO3, WO3) Substituted Silicate Xerogels as Catalysts for the Oxidation of Hydrocarbons with Hydrogen Peroxide," *Journal of Catalysis*, vol. 166, no. 2, pp. 206–217, Mar. 1997, doi: 10.1006/JCAT.1997.1479.
33. E. Caudron, A. Tfayli, C. Monnier, M. Manfait, P. Prognon, and D. Pradeau, "Identification of hematite particles in sealed glass containers for pharmaceutical uses by Raman microspectroscopy," *Journal of Pharmaceutical and Biomedical Analysis*, vol. 54, no. 4, pp. 866–868, 2011, doi: 10.1016/j.jpba.2010.10.023.
34. J. He, Y. Li, D. An, Q. Zhang, and Y. Wang, "Selective oxidation of methane to formaldehyde by oxygen over silica-supported iron catalysts," *Journal of Natural Gas Chemistry*, vol. 18, no. 3, pp. 288–294, 2009, doi: 10.1016/S1003-9953(08)60120-6.
35. A. M. Jubb and H. C. Allen, "Vibrational spectroscopic characterization of hematite, maghemite, and magnetite thin films produced by vapor deposition," *ACS Applied Materials and Interfaces*, vol. 2, no. 10, pp. 2804–2812, 2010, doi: 10.1021/am1004943.
36. P. M. Cuesta Zapata, M. S. Nazzarro, M. L. Parentis, E. E. Gonzo, and N. A. Bonini, "Effect of hydrothermal treatment on Cr-SiO2mesoporous materials," *Chemical Engineering Science*, vol. 101, pp. 374–381, 2013, doi: 10.1016/j.ces.2013.06.041.
37. K. S. W. Sing, "Reporting physisorption data for gas/solid systems with special reference to the determination of surface area and porosity (Provisional)," *Pure and Applied Chemistry*, vol. 54, no. 11, 1982, doi: 10.1351/pac198254112201.
38. C. Perego and P. Villa, "Catalyst preparation methods," *Catalysis Today*, vol. 34, pp. 281–305, 1997.
39. G. Gómez Millán, Z. El Assal, K. Nieminen, S. Hellsten, J. Llorca, and H. Sixta, "Fast furfural formation from xylose using solid acid catalysts assisted by a microwave reactor," *Fuel Processing Technology*, vol. 182, no. July, pp. 56–67, 2018, doi: 10.1016/j.fuproc.2018.10.013.
40. A. Chatterjee, X. HU, and F. L. Y. Lam, "Modified coal fly ash waste as an efficient heterogeneous catalyst for dehydration of xylose to furfural in biphasic medium," *Fuel*, vol. 239, no. October 2018, pp. 726–736, 2019, doi: 10.1016/j.fuel.2018.10.138.
41. L. Zhang, G. Xi, K. Yu, H. Yu, and X. Wang, "Furfural production from biomass–derived carbohydrates and lignocellulosic residues via heterogeneous acid catalysts," *Industrial Crops and Products*, vol. 98, pp. 68–75, 2017, doi: 10.1016/j.indcrop.2017.01.014.
42. K. Sun et al., "A solid iron salt catalyst for selective conversion of biomass-derived C5 sugars to furfural," *Fuel*, vol. 300, no. March, p. 120990, 2021, doi: 10.1016/j.fuel.2021.120990.
43. "Enhanced adsorption of acetylsalicylic acid over hydrothermally synthesized iron oxide-mesoporous silica MCM-41 composites," *Journal of the Taiwan Institute of Chemical Engineers*, vol. 65, pp. 591–598, Aug. 2016, doi: 10.1016/J.JTICE.2016.06.006.
44. S. Buttha, S. Youngme, J. Wittayakun, and S. Loiha, "Formation of iron active species on HZSM-5 catalysts by varying iron precursors for phenol hydroxylation," *Molecular Catalysis*, vol. 461, no. June, pp. 26–33, 2018, doi: 10.1016/j.mcat.2018.09.016.